M. Giorgetti et al. (Eds.)

doi:10.3233/ATDE240680

Design PID Controller Utilizing the Root Locus Technique for Inspiratory Cycle Volume Control Mode of Two Double-Acting Piston Pump Ventilator

Trung Dat PHAN [a,b], Cong Toai TRUONG [a,b], Van Tu DUONG [a,b], Huy Hung NGUYEN [c] and Tan Tien NGUYEN [a,b,1]

[a] *National Key Laboratory of Digital Control and System Engineering (DCSELab), Faculty of Mechanical Engineering, Ho Chi Minh City University of Technology (HCMUT), Linh Trung Ward, Thu Duc City, Ho Chi Minh City, Vietnam*

[b] *Vietnam National University Ho Chi Minh City, Linh Trung Ward, Thu Duc City, Ho Chi Minh City, Vietnam*

[c] *Faculty of Electronics and Telecommunication, Sai Gon University, Ho Chi Minh City, Vietnam*

Abstract. In epochs of significant fluctuations in human health, medical equipment has garnered unprecedented attention, with mechanical ventilators being a focal point of numerous studies. Previous research has typically focused on controlling two critical parameters: volume and pressure. In actuality, the mechanical ventilator's controller must continuously monitor and address the intricate dynamics of the respiratory, which comprises airflow, pressure, and volume, to operate the two double-acting piston pumps in real time to meet the patients experiencing disease. To surmount this obstacle, this paper puts forward designing a PID controller based on a root locus to modulate the output airflow and ensure the tidal volume remains within a 15% error margin of the actual value. Specifically, simulations were conducted with the parameters of a 70-kilogram male patient in scenarios such as normal lungs, COPD, and ARDS. From there, the result of these scenarios are solid evidence to demonstrate that the airflow follows the square wave signal accurately, and the relative error of the tidal volume is maintained within a 5% error margin. Moreover, this approach markedly improves the transient response and steady-state error of the output airflow compared to the initial system.

Keywords. COVID-19, two double-acting piston pump, inspiratory cycle, volume control.

1. Introduction

The COVID-19 pandemic, which began in late 2019, has dramatically impacted global health systems and highlighted critical shortages in medical equipment, particularly

---

[1] Tan Tien NGUYEN, Corresponding author, National Key Laboratory of Digital Control and System Engineering (DCSELab), Faculty of Mechanical Engineering, Ho Chi Minh City University of Technology (HCMUT), Linh Trung Ward, Thu Duc City, Ho Chi Minh City, Vietnam; E-mail: nttien@hcmut.edu.vn.

mechanical ventilators [1]. In reality, traditional ventilators are often complex and expensive, incorporating advanced features into a wide range of clinical scenarios. However, the sheer tidal volume of patients during the COVID-19 crisis has necessitated the development of simpler, more affordable ventilator designs that can be quickly manufactured [2]. These simpler ventilators [3–6] focus on essential functionalities to provide the necessary respiratory support while being easier to produce and maintain as two double-acting piston pump (DAPP) mechanisms [7, 8]. This configuration offers a robust and efficient means of generating the required airflow for ventilation. The DAPP can deliver air during both the forward and backward strokes, thus improving the efficiency and consistency of the airflow. This simplicity in design makes it an attractive option for creating ventilators that can be rapidly produced at a lower cost.

Currently, mechanical ventilators available on the market have numerous ventilation modes, ranging from simple to complex [9]. Importantly, the controller for a mechanical ventilator must be designed to handle the dynamic nature of respiratory demands by continuously monitoring various parameters such as airflow, pressure, and volume and adjusting the operation of the DAPP in real time to match the patient's needs. Hence, this paper presents the design and development of a controller for a DAPP in inspiratory cycle volume control mode. Prominently, it emphasizes achieving the desired tidal volume through precise control of the inspiratory airflow. The procedure is as follows:

- The mathematical model of the DAPP system and the controller evaluation criteria are established.
- Root locus technique-based compensators are incorporated to ensure the output airflow meets the desired response and steady-state error requirements [10,11].
- The output tidal volume is observed by integrating the airflow at each time step, and the relative error between the actual tidal volume and the desired tidal volume is evaluated.

2. Material and Method

2.1. Overall System Description

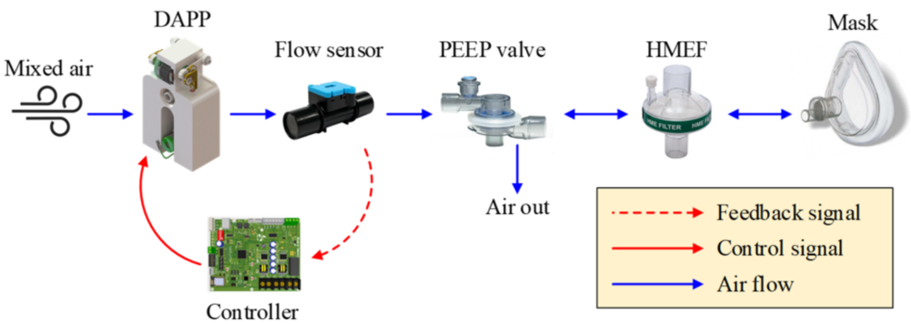

Figure 1. Circuit structure of DAPP.

Figure 1 depicts the structure and operation of the two double-acting pumps (DAPP) system, which is represented significantly in the research paper [8]. Also, in this research paper, the transfer function of the DAPP system is expressed in the frequency domain as follows:

$$G(s) = \frac{Q(s)}{U(s)} = \frac{Ke^{-\theta s}}{\tau s + 1} \tag{1}$$

where $Q(s)$ is the output airflow of the DAPP system in the frequency domain; $U(s)$ is the voltage supplied to the DC motor driver module in the frequency domain; $\tau = 0.03$ is a time constant of the DAPP system; $K = 531$ is the steady state gain; $\theta = 0.04$ is the dead time.

In volume control mode, this paper focuses on regulating the DAPP's airflow to track the desired square wave, meaning that the flow is kept constant throughout the inspiratory cycle. The airflow time is given as follows:

$$Q_d(t) = \frac{V_T RR(IE + 1)}{60IE} = const, 0 \le t \le T_I \tag{2}$$

where $Q_d(t)$ is the desired airflow expressed in ml/s; V_T is the tidal volume expressed in ml; T_I is the inspiratory time expressed in second; RR is the respiration rate expressed in bpm; IE is the inspiratory to expiratory ratio.

The definitions of the ventilator setting parameters are summarized in table 1.

Table 1. Definitions and symbols of the ventilator settings.

Parameters	Symbol	Definition
Tidal volume, ml	V_T	The amount of air delivered to the lungs with each breath
$I{:}E$ ratio	IE	The duration of the inspiratory phase relative to the expiratory phase
Inspiratory time, s	T_I	The period during which inhalation occurs in a respiratory cycle
Respiration rate, bpm	RR	The number of breaths delivered by the ventilator per minute

2.2. Method

The method of designing a Proportional–Integral–Derivative controller (PID controller) based on root locus is applied in this paper. The objective of the PID controller is to modulate the output airflow to follow a square wave profile, as mentioned in [12], and to ensure the tidal volume remains within a 15% error margin of the actual value. Initially, the performance criteria for the controller are outlined. Then, a PD compensator is added to improve the system's transient response. If the steady-state error is not achieved, a PI compensator is added to eliminate this error. The process of tuning the P, I, and D parameters is repeated until the specified criteria are met. Finally, the tidal volume error is evaluated on a 70 kg male patient in three scenarios: normal lungs, COPD, and ARDS (shown in figure 2).

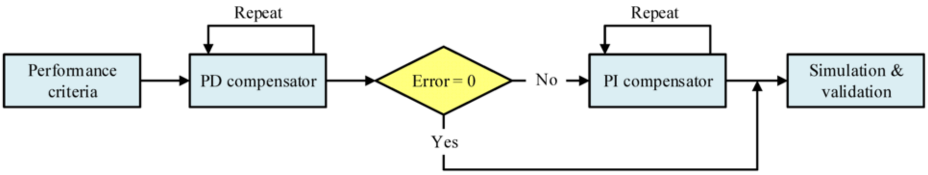

Figure 2. Controller design process using root locus technique.

3. Controller Design

The performance criteria for transient response, steady-state error of the airflow, and relative error of the tidal volume are set as follows:

- Overshoot: $\%OS \leq 10\%$
- Settling time: $T_s \leq 0.1\ s$
- Steady-state error: $e_{ss} \approx 0$
- Relative error of the tidal volume: $\delta \leq 5\%$

The overall control scheme is described in figure 3.

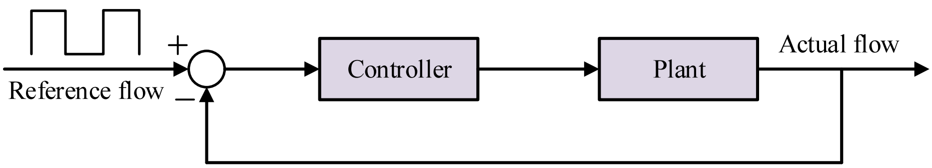

Figure 3. Square flow control scheme for DAPP system.

Applying the Taylor approximation formula with a small θ, Equation (1) can be rewritten as:

$$G(s) \approx \frac{K}{(\tau s + 1)(\theta s + 1)} = \frac{442500}{(s + 25)\left(s + \frac{100}{3}\right)} \tag{3}$$

From $\%OS$ and T_s values, the desired poles postion can be found by this formular:

$$\begin{cases} \%OS \leq 10\% \rightarrow \zeta \geq \dfrac{-\ln(\%OS)}{\sqrt{\pi^2 + \ln^2(\%OS)}} = 0.59 \rightarrow \zeta = 0.6 \\ T_s \leq 0.1 \rightarrow \omega_n \geq \dfrac{4}{T_s \zeta} = 66.67 \rightarrow \omega_n = 70 \end{cases} \tag{4}$$

Thus, the dominant pole pair is determined as $s^* = -\zeta\omega_n \pm j\omega_n\sqrt{1-\zeta^2} = -42 \pm 56j$

3.1. PD Compensator Design

The transfer function of the PD compensator is defined as follows:

$$G_{PD}(s) = K_P + K_D s = K_D\left(s + \frac{K_P}{K_D}\right) = K_D(s + p_3) \tag{5}$$

where $p_3 \triangleq K_P/K_D$.

The required phase compensation angle is calculated by referring to figure 4

$$\phi = -180° + 106.89° + 98.8° = 25.69° \tag{6}$$

From the phase compensation angle in Equation (6), the pole position p_3 is determined by:

$$p_3 = \frac{56}{\tan\phi} + 42 = 158.41 \tag{7}$$

The gain K_D is determined in such a way that the following condition holds:

$$|G_{PD}(s)G(s)|_{s=s^*} \tag{8}$$

Substitute (3), (5) and s^* into (8), we have:

$$\left|K_D(s + 158.41)\frac{442500}{(s+25)\left(s+\frac{100}{3}\right)}\right|_{s=-42\pm 56j} = 1 \tag{9}$$

From Equation (9), the value of K_D is obtained:

$$K_D = 5.8 \times 10^{-5} \tag{10}$$

The value of K_P is determined by the value of p_3:

$$K_P = p_3 K_D = 9.19 \times 10^{-3} \tag{11}$$

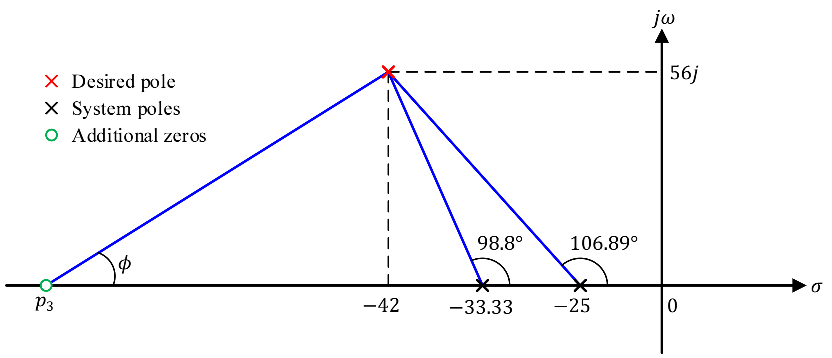

Figure 4. The zero position satisfies the desired transient response.

3.2. PI Compensator Design

The transfer function of the PI compensator is defined as:

$$G_{PI}(s) = K_{P'} + \frac{K_I}{s} = \frac{K_{P'}(s + p_4)}{s} \tag{12}$$

where $p_4 \triangleq K_I/K_{P'}$.

To maintain the transient response of the system, the zero should be chosen as close as possible to the origin relative to the real part of the dominant pole pair. Therefore, one can choose $p_4 = 0.1$, as shown in figure 5.

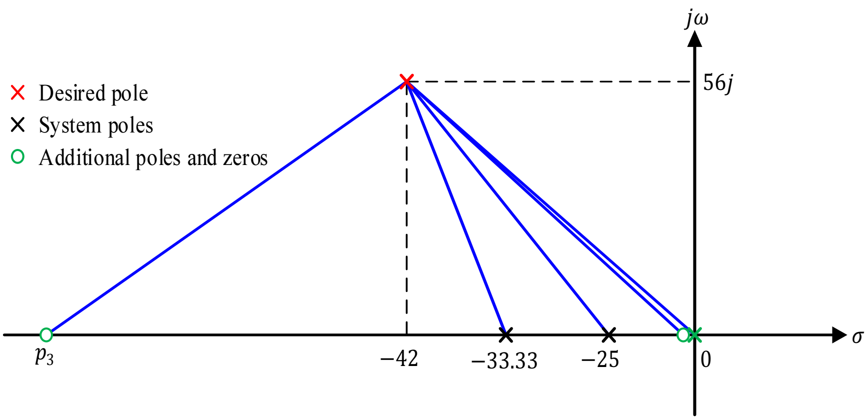

Figure 5. The zero and pole positions for eliminating the steady-state error.

Using the condition of Equation (8), the following expression can be obtained

$$K_{P'} \frac{(5.8 \times 10^{-5}) \times 442500 \times 129.17 \times 69.94}{56.67 \times 58.52 \times 70} = 1 \tag{13}$$

From Equation (13), the value of $K_{P'}$ is derived:

$$K_{P'} = 1 \tag{14}$$

Consequently, the value of K_I is determined from p_4 and $K_{P'}$:

$$K_I = p_4 K_{P'} = 0.1 \tag{15}$$

The values of the three parameters K_P, K_I, and K_D yield

$$\begin{cases} K_P = 9.19 \times 10^{-3} \\ K_I = 0.1 \\ K_D = 5.8 \times 10^{-5} \end{cases} \tag{16}$$

4. Results and Discussion

Figure 6 shows the root locus of the system after implementing the PID controller. It can be seen that the PID controller directs the system's root locus through the desired pole pair. Figure 7 illustrates the DAPP ventilator's response before and after the PD and PI compensators were implemented. It can be observed that before implementing the compensators, the open-loop plant response exhibited a dramatic overshoot (the airflow over $15 l/s$) and the airflow could not reach the steady-state value, continuously oscillating around the reference with a certain amplitude (with an oscillating value greater than the value reference between 0.95% and 36.24%). When the PD compensator was added, the PD Controller curve response improved significantly with an overshoot of 9.1% and a settling time of 0.09 seconds, but the DAPP ventilator still had a steady-state error of 17% . Finally, the PI compensator was added to make the steady-state error converge to zero while maintaining the settling time and overshoot achieved by the PD compensator.

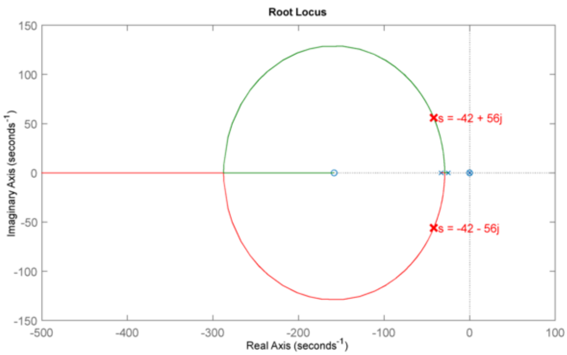

Figure 6. Root locus of the ventilator plant after implementing the PID controller.

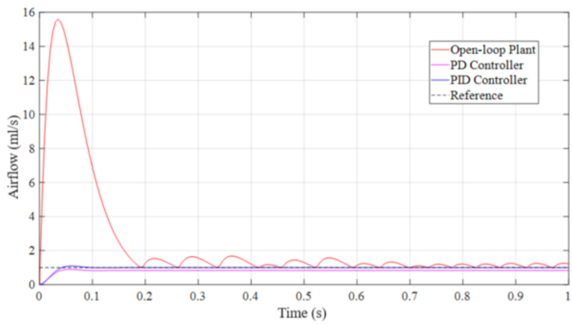

Figure 7. System response with step input before and after implementing the PD, PI compensator.

After verifying the system's response to a step input, simulations were applied to specific clinical scenarios. Simulation is conducted on a $70\ kg$ male patient with airway resistance R and compliance C values of $10\frac{cmH_2O}{l/s}$, and $0.05\frac{l}{cmH_2O}$, respectively. Figure 8 shows the airflow and tidal volume graphs for the first four respiratory cycles under three different scenarios corresponding to three respiratory conditions: normal lungs, COPD, and ARDS. In all three scenarios, the flow is controlled to track a square wave signal defined by Equation (2) and maintained for the duration T_I in the inspiratory cycle. Consequently, the tidal volume during inspiratory phase also increases linearly following a ramp function. During the expiratory cycle, the system ceases to supply airflow, and the airflow is expelled out, with the tidal volume decreasing exponentially because of the elastic properties of the lungs.

Additionally, the results shown in table 2 indicate that the system meets the initial control criteria effectively, with an airflow overshoot of less than 10%, a flow settling time of less than 0.1 s, and a steady-state error close to zero. Furthermore, the relative error of the tidal volume remains below 5% of the desired value. Specifically, the relative errors for tidal volume in the normal lungs, COPD, and ARDS scenarios are 1.7%, 1.93%, and 0.68%, respectively.

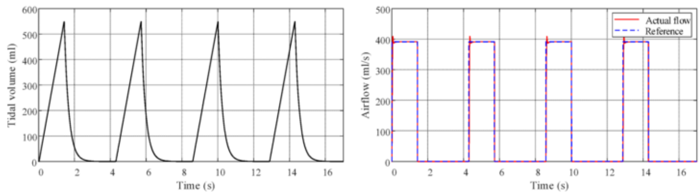

a) Tidal volume, airflow waveform in normal lungs scenario, $V_T = 560\,ml,\ T_I = 1.43\ s, Q_d = 391.61\frac{ml}{s}, IE = \frac{1}{2}$

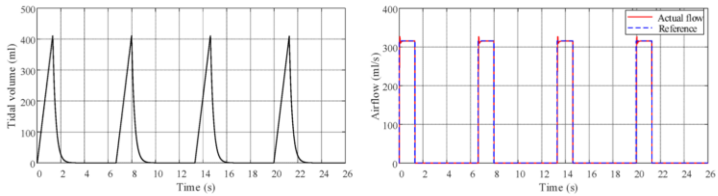

b) Tidal volume, airflow waveform in COPD scenario, $V_T = 420\,ml, T_I = 1.33\ s, Q_d = 315.79\frac{ml}{s}, IE = \frac{1}{4}$

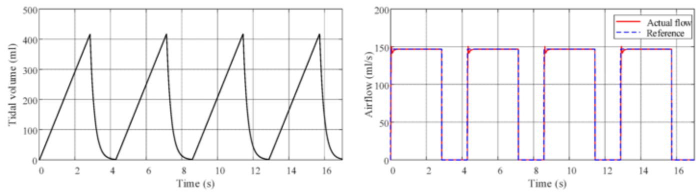

c) Tidal volume, airflow waveform in ARDS scenario, $V_T = 420\,ml, T_I = 2.86\ s, Q_d = 146.85\frac{ml}{s}, IE = 2{:}1$

Figure 8. Simulation results of volume and flow waveform in three clinical scenarios.

Table 2. Simulation performance in three clinical scenarios

	Normal lungs	COPD	ARDS
Tidal volume performance			
Desired tidal volume, ml	560	420	420
Actual tidal volume, ml	550.48	411.89	417.13
Relative error, %	1.7	1.93	0.68
Airflow performance			
Overshoot, %	4.44	3.51	2.5
Settling time, s	0.08	0.07	0.09
Steady-state error, ml/s	≈0	≈0	≈0

5. Conclusion

The paper dedicated a method for designing a PID controller for the inspiratory cycle of a DAPP using the root locus technique. The PID controller is designed based on the system's transfer function and ventilation parameters specified in Vietnam standards TCVN 7010-2-2007. The addition of the controller significantly improves the transient response and steady-state error of the output flow compared to the original system. Furthermore, simulation results in three different scenarios demonstrate that the airflow follows the square wave signal accurately, and the relative error of the tidal volume does not exceed the 5% error.

Nevertheless, the paper exhibits certain limitations, including omitting considerations regarding flow sensor noise. Otherwise, the noise can significantly impact the effectiveness of the designed controller. Therefore, the signal of the flow sensor needs to be analyzed and appropriately filtered in future work. In the future, DAPP is going to update comprehensive factors which comprise the hardware and the control mode to adapt to various patient breathing problems.

Acknowledgments

This research is funded by Vietnam National University Ho Chi Minh City (VNU-HCM) under grant number TX2024-20b-01. We acknowledge the support of time and facilities from National Key Laboratory of Digital Control and System Engineering (DCSELab), Ho Chi Minh City University of Technology (HCMUT), VNU-HCM for this study.

References

[1] Bown CP. How COVID-19 medical supply shortages led to extraordinary trade and industrial policy. Asian Economic Policy Review. 2022; 17: 114–135.
[2] Fang Z, Li AI, Wang H, Zhang R, Mai X, Pan T. AmbuBox: A fast-deployable low-cost ventilator for COVID-19 emergent care. SLAS Technol. 2020; 25: 573–584.
[3] Truong CT, Huynh KH, et al. Characteristic of paddle squeezing angle and ambu bag air volume in bag valve mask ventilator. The 17th International Conference on Intelligent Unmanned Systems. 2021.
[4] Truong CT, Huynh KH, Duong VT, Nguyen HH, Nguyen TT. Model free volume and pressure cycled control of automatic bag valve mask ventilator. AIMS Bioengineering. 2021; 8(3): 192–207.
[5] Truong CT, Nguyen KD, Duong VT, et al. Model identification of two double-acting pistons pump a NARX network approach. International Conference on Ubiquitous Robots. 2023.
[6] Truong CT, Huynh KH, Duong VT, Nguyen HH, Pham LA, Nguyen TT. Linear regression model and least square method for experimental identification of AMBU bag in simple ventilator. International Journal of Intelligent Unmanned Systems. 2022.
[7] Robert R, Micheau P, Cyr S, Lesur O, Praud JP, Walti H. A prototype of volume-controlled tidal liquid ventilator using independent piston pumps. ASAIO Journal. 2006; 52: 638–645.
[8] Nguyen DK, Truong CT, Duong VT, Nguyen HH, Nguyen TT. Model identification of two double-acting pistons pump. Journal of Advanced Marine Engineering and Technology. 2023: 59–65.
[9] Chatburn RL, Mireles-Cabodevila E. Closed-loop control of mechanical ventilation: Description and classification of targeting schemes. Respir. Care. 2011; 56: 85–98.
[10] Nise N. Control Systems Engineering. John Wiley & Sons. 2011.
[11] Basilio JC, Matos SR. Design of PI and PID controllers with transient performance specification. IEEE Transactions on Education. 2002; 45: 364–370.
[12] Tamburrano P, Sciatti F, Distaso E, Di Lorenzo L, Amirante R. Validation of a simulink model for simulating the two typical controlled ventilation modes of intensive care units mechanical ventilators. Applied Sciences (Switzerland). 2022; 12.